A novel sensitive cell-based love wave biosensor for marine toxin detection

Xi Zhang, Jiaru Fang, Ling Zou, Yingchang Zou, Lang Lang, Fan Gao, Ning Hu, Ping Wang

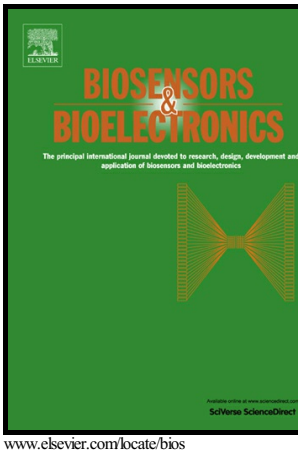

www.elsevier.com/locate/bios

PII: S0956-5663(15)30310-9
DOI: http://dx.doi.org/10.1016/j.bios.2015.07.062
Reference: BIOS7880

To appear in: *Biosensors and Bioelectronic*

Received date: 23 May 2015
Revised date: 22 July 2015
Accepted date: 27 July 2015

Cite this article as: Xi Zhang, Jiaru Fang, Ling Zou, Yingchang Zou, Lang Lang Fan Gao, Ning Hu and Ping Wang, A novel sensitive cell-based love wave biosensor for marine toxin detection, *Biosensors and Bioelectronic* http://dx.doi.org/10.1016/j.bios.2015.07.062

A Novel Sensitive Cell-based Love Wave Biosensor for Marine Toxin Detection

Xi Zhang, Jiaru Fang, Ling Zou, Yingchang Zou, Lang Lang, Fan Gao, Ning Hu*, Ping Wang*

Biosensor National Special Lab, Key Lab for Biomedical Engineering of Ministry of Education, Department of Biomedical Engineering, Zhejiang University, 310027 Hangzhou, China.

**Corresponding author Tel: +86 571 87952832; fax: +86 571 87952832*

E-mail: cnpwang@zju.edu.cn (Ping Wang), *huning@zju.edu.cn* (Ning Hu)

Abstract

A novel HepG2 cell-based biosensor using Love Wave sensor was developed to implement the real-time and sensitive detection of a diarrheic shellfish poisoning (DSP) toxin, Okadaic acid (OA). Detachable Love Wave sensor unit and miniaturized 8-channel recording instrument were designed for the convenient experimental preparation and sensor response signal measurement. The Love Wave sensor, whose synchronous frequency is around 160 MHz, was fabricated with ST-cut quartz substrate. To establish a cell-based biosensor, HepG2 cells as sensing elements were cultured onto the Love Wave sensor surface, and the cell attachment process was recorded by this biosensor. Results showed this sensor could monitor the cell attachment process in real time and response signals were related to the initial cell seeding densities. Furthermore, cell-based Love Wave sensor was treated with OA toxin. This biosensor presented a good performance to various OA concentrations, with a wide linear detection range (10-100 μg/L). Based on the ultrasensitive acoustic wave platform, this cell-based biosensor will be a promising tool for real-time and convenient OA screening.

Key words: Love Wave sensor; Okadaic acid (OA); Cell attachment; Cell-based biosensor.

1. Introduction

Okadaic acid (OA) is produced by some unicellular algae from plankton and benthic microalgae. This kind of marine toxin accumulates in the digestive glands of shellfish without resulting in any toxic effect on the bivalves (Sassolas et al. 2013). However, when humans consume a sufficient amount of contaminated seafood, gastrointestinal troubles known as diarrheic shellfish poisoning (DSP) occurs. The action mechanism of OA is based on the inhibition of protein phosphatases and enzymes which play a major role in protein dephosphorylation in cells. These toxins bind to the receptor sites of protein phosphatases type 1 (PP1) and 2A (PP2A), and block their activity. Consequently, hyperphosphorylation of the proteins that control sodium secretion by intestinal cells will happen. Meanwhile, hyperphosphorylation of cytoskeleton or junctional moieties that regulate solute permeability is favored. All these can cause a sodium release and a subsequent passive loss of fluids, which is responsible for the diarrheic symptoms (Aune and Yndestad 1993). Besides, some studies carried out on animals have identified OA as a tumor promoter and also proved its mutagenic and immunotoxic effects (Campàs et al. 2007). Therefore, it is essential to develop sensitive and reliable methods to detect OA in order to guarantee the seafood safety and minimize the potential risk to human health.

In vivo mouse bioassay is widely used for marine toxins detection. Although it can provide an indication about the overall toxicity of the sample, results derived from this method are poorly accurate, non- or semi-quantitative. Apart from being laborious and time-consuming, the mouse bioassay also goes against the ethic. In order to replace the mouse bioassay, various biosensors have been developed and utilized as the analytical tools for preliminary screening the sample toxicity. Among these, cell-based biosensors have been designed as a promising biological

alternative method recently (Giaever and Keese 1991; Giaever and Keese 1993). As we all know, living cells are extremely sensitive to modulations or disturbances in physiological microenvironment, so they could be utilized to screen pharmaceutical drugs or environmental agents which might cause perturbations or apoptosis of cells (Liu et al. 2014). By employing living cells as sensing elements combined with sensors or transducers, cell-based biosensors could monitor the metabolism, impedance and excitability of cells in the presence of various analytes including pathogens, chemical pollutants, toxic chemicals, or drugs *in vitro* (Ahmad and Moore 2009; Yicong et al. 2001).

Over the last decades, an increasing number of scientific reports which are concerned with the cell-based biosensors established by the piezoelectric acoustic sensors have attracted the growing interests for this technology. In contrast to the cellular impedance biosensors, the piezoelectric acoustic sensor detection is restricted to the modifications occurring in the cell-substrate interaction and do not take into account the cell-cell contacts (Nowacki et al. 2015; Wegener et al. 2001). This makes the piezoelectric acoustic sensors, especially the quartz crystal microbalance, be widely used for cell-surface interaction studies, such as attachment and spreading (Saitakis and Gizeli 2012; Saitakis et al. 2010; Wegener et al. 1998; Xi et al. 2013). Furthermore, cell responses to some reagent measured by acoustic sensors were studied lately (Higashiyama et al. 2014; Otori et al. 2013; Racz et al. 2011).

To date, published examples of cell response measurement based on surface acoustic wave sensor are rare, in particular with long-term cell growth process monitoring through the Love Wave sensor. Moreover, piezoelectric acoustic sensors have been reported for marine toxin detection recently, which utilized the quartz crystal microbalance and Love Wave sensor as

immunosensors (Fournel et al. 2012; Tang et al. 2002). The main drawbacks of these immunosensors are large detection limit as well as the complicated reagents preparation and pretreat processes. In this study, a sensitive and convenient cell-based Love Wave sensor for OA detection is presented here. The Love Wave sensor, whose synchronous frequency is around 160 MHz, was fabricated with ST-cut quartz substrate. HepG2 cell lines were cultured onto the sensor surface as the sensing elements. Besides, a portable and miniaturized instrument was designed in order to implement the real-time and multi-channel synchronous detection. With this system, sensor responses to the cell attachment and OA were investigated, respectively.

2. Materials and methods

2.1 Reagents

DMEM medium (Dulbecco's modified eagle medium) with high glucose, fetal calf serum (FBS), 0.25% Trypsin-EDTA, and phosphate buffered saline (PBS) were obtained from Gibico, USA. OA (Sigma, USA) stock solution was prepared in DMSO and filtered with 0.22 μm membrane filter unit (Millipore, USA). OA was diluted by DMEM medium with high glucose when it is used to treat with cells.

2.2 Love Wave sensors

In the present study, the Love Wave sensor (Fig. 1 (a)) is consisted of a piezoelectric quartz substrate (ST cut). 20/200 nm thick Ti/Au interdigitated transducers (IDTs) are deposited onto the quartz substrate in order to generate pure shear horizontal acoustic waves propagating perpendicular to the X crystallographic axis. The input and output IDTs electrodes are comprised

of 50 split-finger pairs with a wavelength λ = 28 μm, which determines the center frequency of the sensor to be around 160 MHz (Matatagui et al. 2013; Zhang et al.). The spacing center to center between IDTs is 200λ and the acoustic aperture is 75λ. Afterwards, the IDTs patterned substrate is guided with a 3 μm SiO_2 film deposited by plasma enhanced chemical vapor deposition (PECVD), which confines the acoustic wave energy near the sensing surface and realizes the Love Wave mode. Wegener and colleagues have demonstrated that the cells preferred attaching on gold surface than quartz (Wegener et al. 1998). Therefore, to improve the cell attachment on the sensor surface, 200 nm Au layer is deposited on top of guiding layer and the location is right between the input and output IDTs.

Fig.1

2.3 Measurement system

To implement the cell growth on the sensor surface, a polydimethylsiloxane (PDMS) chip is designed and used as the cell culturing chamber. Fig. 2 (a) illustrates the scheme of the Love Wave sensor assembled with the PDMS chip. The chip is composed of four air cavities and two large liquid storage cavity. These air cavities could protect the IDTs and eliminate the electric influence of the liquid efficiently (Rocha et al. 2013). The liquid storage cavity is right in the middle of the air cavities, the height and volume of this cavity are about 12 mm and 150 μL, respectively. Cells and culture medium are injected in and removed from this liquid storage cavities with a micropipette. Before each experiment, the PDMS chip is mounted on the sensor surface tightly by a plexiglass plate and two screws (Fig. 2 (b)), so that liquids could only stay in the large storage

cavity without any leakage to the air cavities.

Fig.2

To establish the multi-channel Love Wave sensor detection system for working in the CO_2 incubator, a portable and miniaturized instrument is employed here instead of the bulky network analyzer (Fig. 1 (b)). The basic detection principle and circuit design of the instrument have been described elsewhere (Montagut et al. 2011; Zhang et al. 2014). By means of this circuit, both the insertion loss and phase signals of sensors can be measured. The Love Wave sensor array assembled with PDMS chips is mounted on a custom-made metal holder, which is located on top of the instrument, and the sensor array is connected to the detection interface of the instrument by shielded cables. Then sensor signals are processed by the circuit and the detection results are converted via a multi-channel 16-bit ADC chip (AD7792) with high precision. After this electrical outputs converting procedure, information about both the insertion loss and phase of sensors can be obtained by the MCU. Ultimately, data stored in the MCU are sent to the PC through serial communication and recorded by the LabVIEW software which was programmed specifically for this experiment. With this measurement system, responses of 8-channel Love Wave sensor array could be recorded in real-time and continuously.

2.4 Cell culture

HepG2 cell line, kindly provided by Dr. Wu (School of Medicine, Zhejiang University, Hangzhou, China) were cultured in Roswell Park Memorial Institute (RPMI)-DMEM medium with 10% heat inactivated FBS and 0.5% antibiotic solution (10 mg/mL streptomycin and 1000

U/mL penicillin) at 37 °C in humidified air with 5.0% CO_2 in an incubator (Thermo Fisher Scientific, USA). The medium was changed every 1-2 days, and cells were detached from the culture flask by using 0.25% Trypsin-EDTA solution after it reached the confluence of 80%.

2.5 Experiment setup

2.5.1 Cell attachment measurement

To demonstrate that the Love Wave sensors together with the detection system can be directly utilized to monitor the cell attachment, HepG2 cells were detached from the culture flask and 100 μL cell suspensions with different cell seeding densities were prepared. Before cell culture, sensor surfaces were immersed in cell dissociation buffer for 30 min. Then sensor chips were rinsed with deionized water and dried under pure nitrogen gas. After that, these chips were assembled with the PDMS chips, and HepG2 cell suspensions with different cell densities were seeded into the liquid storage cavities. After the cell seeding, both the sensors and the detection system were placed inside a CO_2 incubator. Meanwhile, the detection system started to measure the cell growth curves and the insertion loss as well as the phase signals of each sensor were recorded once every ten seconds during the whole procedure. After cells were cultured for 24 h, the medium of each liquid storage cavity was removed, and then the cell status was observed by a stereo microscope (Sharp Inc., Japan).

2.5.2 Real-time monitoring of cellular response to marine toxins

In the toxin detection experiment, 100 μL of HepG2 cell suspensions with the same cell seeding density were added onto the sensor surface. After cell seeding, the sensor chips, as well as

the detection system, were placed in the incubator. Before exposure to toxins, the whole sensor preparation and cell seeding processes here were consistent with the cell attachment monitoring experiment. And cells cultured in each wells also needed to be monitored by the detection system for 24 h continuously. Then the medium of treated groups was removed and replaced by 100 μL fresh medium with OA. While the medium of the control group was removed and replaced by 100 μL fresh medium without any toxin. When all these steps were finished, the sensor array was placed back to the CO_2 incubator and the measurement was performed for another 12 h.

3. Result and discussion

3.1 Dynamically monitoring of cell attachment and cell seeding number decision

To verify our system could be applied to detect the cell attachment process directly, HepG2 cells were detached from the culture flask and inoculated onto the sensor chip at 2000, 4000, 6000, 8000, 10,000 and 12,000 cells/well. Cell growth curves of 8 wells were measured and recorded by the detection system for 24 h after cell seeding. Fig. 3 (a) and (b) shows the real-time growth curves of HepG2 cells measured by the system with different cell densities ranging from 2000 to 12,000 cells/well. At the time of zero, both the insertion loss and the phase signal values with different seeding densities were all set to be zero, which means no cell was attached onto the sensor surface at the beginning of the experiments. Along with the incubation time increased, the insertion loss and phase values started to drop. And from Fig. 3 (a) and (b), it is obvious that signals descend, fluctuated and unchanged sequentially by contacting with HepG2 cells, corresponding to the initial, transitional and final phases in cell attachment. Curves decreased greatly during the first four hours. And for almost all the seeding densities, the signal shifts

reached the maximum after about 4 h, followed by steady curves. During the next twenty hours, the remaining signals became much stable or showed a slow decreasing tendency, which has a significant difference with the former ones. This phenomena is consistent with other reported literatures, which present detection results of quartz crystal microbalance in response to HepG2 cells (Wei et al. 2007; Wei et al. 2011). The reason for this might be that cells in cell suspensions deposited onto the sensor surface in the first place, once the suspensions were added into the cell culturing chamber. Cells attachment is a complex process, since cells do not interact directly with the surface of a man-made substrate but with a pre-adsorbed layer of extracellular biomolecules, mostly proteins from the extracellular matrix (ECM) (Liu et al. 2014). During the cell-substrate attachment procedure, cells come into contact with the substrate, attach loosely, and flatten over the substrate surface. Simultaneously, cells form attachment complexes that connect the ECM with intracellular action filaments (stress fibers) through integrin (Geiger and Zaidel-Bar 2012). So in this stage, ECM layers were formed between cells and sensor surface, and cells completed the process of attachment (the initial phase, 0-4 h). In the following stage, attached cells started to proliferate, which was a much slower procedure, and the gravimetric change of the proliferation was smaller than that of the attachment. Consequently, signals became stable gradually. Besides, there were some signal fluctuations in detection curves, which might be caused by cell detachment and re-attachment (Wei et al. 2011).

When cells attached and flattened onto the acoustic path, acoustic waves would be interrupted by these cells, which induced inevitable acoustic attenuation. As is obvious in Fig. 3 (a) and (b), the shifts of two Love Wave sensor parameters, insertion loss and phase, are dependent on the number of cells that were seeded onto the sensor surface. Since cells almost completed their

attachment process at the end of the initial phase and cells began to proliferate afterwards, we think signals measured at 4th hours during the experiment should be regarded as the responses to the cell seeding densities. Therefore, values at the 4th hours were extracted from the measured curves, and the dependence of different HepG2 cell seeding densities versus these values are shown in Fig. 3 (c) and (d). For the insertion loss, the signal shift ranges from 0.95 dBm for 2000 cells/well to about 5 dBm if 12,000 cells/well was seeded. While for the phase, the signal varies from 17.5 degrees for 2000 cells/well to 34.4 degrees for 12,000 cells/well. The graph indicates that higher cell seeding density produced larger signal shifts. And it is shown that both the insertion loss and the phase drifts are linear with the cell seeding densities. The linear correlation coefficients are 0.9508 for the insertion loss and 0.8484 for the phase drift, respectively. It is obvious that the insertion loss shows a better linear relationship than the phase drift, which indicates that the signal variations are mostly due to viscoelastic changes close to the sensor surface. It can be used to verify that cells don't exhibit pure mass-load behavior and attached cells on the substrate behave more like a viscoelastic material than a rigid mass film, which has been reported by others (Fohlerová et al. 2007; Li et al. 2008; Saitakis and Gizeli 2012; Wegener et al. 2000). In addition, according to this results, only the insertion loss signals were measured for the following toxin detection experiment since the insertion loss could reflect cell growth condition better than the phase signal.

Fig.3

As demonstrated by Fig. 3, the number of initial seeding cells shows apparent influences on the output of sensor signal. Therefore, it is important to optimize the number of initial seeding

cells in order to establish a sensitive cell-based biosensor for the further marine toxin detection. Both the insertion loss and the phase at low cell density decreased slowly and their shifts were relatively small, which result in a low sensor output signal and low sensitivity. On the contrary, these two parameters decreased more quickly and ultimate shifts became larger with the increase of the seeding number. However, there might be some other problems if the initial seeding density is too large. Along with the attachment and proliferation of cells, cells growth will plateau gradually due to exhaustion of the medium or contact inhibition (van Meerloo et al. 2011). Since the cell incubation time of the cell-based assay is 24 h for marine toxins detection, it needs to be ensured that cells are good and their growth should not be inhibited with specific seeding density after long-term culturing. It is difficult to tell the differences of the cell growth situation between each seeding densities only from the detection curves. Hence, sensors with cells on their surface were observed by the stereo microscope and images of cells were taken after cells were cultured for 24 h. Fig. 4 shows the cell growth situation on the sensor chips. It is apparent that the number of cells attached on the sensor surface increased with the increasing of the initial seeding density except the last one. For the last sensor which was seeded with 12,000 cells at first, the cell apoptosis phenomena could be observed obviously. This should be attributed to the exhaustion of the medium as mentioned above. Based on the obtained results and analysis, 10,000 is the suitable seeding number to obtain a better cell-based biosensor.

Fig.4

3.2 Real-time monitoring cell response to OA

Before adding marine toxins, Love Wave sensors seeded with HepG2 cells (10,000 cells/well) were placed in the incubator for 24 h. After that, different concentrations of OA were tested by the Love Wave biosensors and detection signals were recorded for another 12 h. Fig. 5 (a) shows the real-time insertion loss variation curves, which reflect the cell activity changes due to the treatment of 200 μg/L OA and fresh medium. In the first 24 h, two detection curves drop at first and the variation values at the 4^{th} hour are all about 3.5 dBm, which are all in accordance with the results of the cell attachment experiment introduced above. After cells were cultured for 24 h, the former medium of the detection channel was replaced by the medium with OA, while that of the reference channel was replaced by the fresh medium. OA is a powerful inhibitor of phosphatases type 1 and 2A, which affect phosphorylation and dephosphorylation of protein imbalance. The continuous phosphorylation of cytoskeletal protein will lead to the cytoskeleton damage and result in abnormal cell morphology or even cell death with OA concentration dependence (Zou et al. 2014). Consequently, cell morphology changes induced by OA would influence the cell attachment on sensors. From Fig. 5 (a), it is obvious that insertion loss signal of detection channel started to rise once OA was added and become stable after OA introduction for about 4 h. This demonstrates that OA in the medium could influence the normal cell growth process and even cause cell death with high concentration, which would affect the sensor outputs. On the contrary, there was no significant shift for the reference channel signal. This verified that this cell-based biosensor could be utilized for marine toxin detection.

As shown in Fig. 5 (a), detection curves measured from different sensors could hardly start from the same insertion loss value. So it is difficult to distinguish different concentrations OA

only with the raw data recorded by the detection system. In order to solve this problem, the normalization method was adopted here. Hence, data at the 24th hour were extracted and the whole detection curves were divided by these data. By this means, the point at the 24th hour, which was measured right before adding the toxin, is set to be -1. And all the following insertion loss values could start from the unified point, which makes it convenient to compare the differences of the insertion loss variations between different OA concentrations. Fig. 5 (b) shows the normalized curves of HepG2 cells responding to various concentrations of OA (10, 20, 40, 60, 100, 150 and 200 μg/L). From Fig. 5 (b), insertion loss variations of 10-100 μg/L groups could distinguish from each other obviously. While there are only a little bit of differences between 100, 150 and 200 μg/L groups. The reason for this might be that most of attached HepG2 cells were dead and left away from sensor surface after 4 hours in presence of the high concentration OA (above 100 μg/L). Fig. 5 (c) shows the correlation curve and equation for different OA concentrations and the insertion loss variations induced by the corresponding OA. A linear relationship is found between the concentration of OA (10-100 μg/L) and the insertion loss variations with a correlation coefficient of 0.9834.

Fig.5

3.3 Specificity of cell-based biosensor

In order to evaluate the specificity of this cell-based biosensor to OA, the insertion loss variations induced by other marine toxins were measured by the detection system. Besides OA, other two marine toxins tested here were saxitoxin and brevetoxin, respectively. Each toxin was

tested for three times. Saxitoxin (STX) is one of the paralytic shellfish poisoning (PSP) toxins, and it can affect the propagation of the action potential by blocking sodium channels, which will change the membrane potential on a cellular level and cause neurological symptoms in human (Wiese et al. 2010). Brevetoxin (PbTx-3) is a kind of neurologic shellfish poisoning (NSP) toxins which induces the enhancement of sodium inflow into cells (Campàs et al. 2007). The concentrations of OA, STX and PbTx-3 applied in this specificity assay were 100 μg/L. From the results shown in Fig. 6, it is obviously that the insertion loss variation caused by OA was significantly higher than that caused by other two toxins. The variation caused by OA is about 0.929±0.218 dBm, while variations induced by STX and PbTx-3 are 0.212±0.041 dBm and 0.327±0.136 dBm. Therefore, it can be concluded that this cell-based Love Wave biosensor presented a good specificity for OA detection.

Fig.6

These results validate this brand-new biosensor based on Love Wave sensor could be applied for marine toxin detection with high sensitivity, selectivity and wide detection range. Compared with traditional piezoelectric biosensors based on immunological reaction, such as quartz crystal microbalance (Tang et al. 2002), this cell-based biosensor has comparative advantages in wide detection range, low detection limit, as well as convenient reagent preparation and pretreat processes. Besides, unlike cell-based impedance sensors, detection elements of the Love Wave sensor is the acoustic rather than the electrical signal, which is totally harmless to cells cultured on sensor surface. So this kind of biosensor is much more suitable for cell morphology detection and some other applications, which we would study in the future.

4. Conclusion

In this paper, we proposed a novel HepG2 cell-based Love Wave sensor system for the detection of OA. Besides that, sensor responses to the cell attachment process were also investigated. This marine toxin detection method has obvious advantages in OA preliminary screening through combining cell-based assay and real-time, noninvasive monitoring technology. The application of this method reduces the number of animals required and obtains a higher sensitivity than the mouse bioassay. And comparing with previous acoustic wave immunosensors, it not only simplified the detection procedure but also ensure a wide linear detection range (10-100 μg/L). Before this analytical method become practical and be accepted as an alternative method to the mouse assay, there are still a lot of problems need to be solved. As we keep on our research into this cell-based Love Wave sensor and its applications, we hope this system will be a promising solution for marine toxin detection.

Acknowledgments

This work was supported by grants from the National Public Welfare Project of China (No. 201305010), the project of Science and Technology Department of Zhejiang Province of China (No. 2013C93044-2), High-level Personnel Training Project of Cooperation Improvement of America and Oceania Region (No. 20142029), and China Postdoctoral Science Foundation (No. 2015M570511).

References

Ahmad, A., Moore, E.J., 2009. Comparison of Cell-Based Biosensors with Traditional Analytical Techniques for Cytotoxicity Monitoring and Screening of Polycyclic Aromatic Hydrocarbons in the Environment. Analytical Letters 42(1), 1-28.

Aune, T., Yndestad, M., 1993. CHAPTER 5 - Diarrhetic Shellfish Poisoning. In: Falconer, I.R. (Ed.), Algal Toxins in Seafood and Drinking Water, pp. 87-104. Academic Press, San Diego.

Campàs, M., Prieto-Simón, B., Marty, J.-L., 2007. Biosensors to detect marine toxins: Assessing seafood safety. Talanta 72(3), 884-895.

Fohlerová, Z., Skládal, P., Turánek, J., 2007. Adhesion of eukaryotic cell lines on the gold surface modified with extracellular matrix proteins monitored by the piezoelectric sensor. Biosensors and Bioelectronics 22(9–10), 1896-1901.

Fournel, F., Baco, E., Mamani-Matsuda, M., Degueil, M., Bennetau, B., Moynet, D., Mossalayi, D., Vellutini, L., Pillot, J.P., Dejous, C., Rebière, D., 2012. Love wave biosensor for real-time detection of okadaic acid as DSP phycotoxin. Sensors and Actuators B: Chemical 170(0), 122-128.

Geiger, T., Zaidel-Bar, R., 2012. Opening the floodgates: proteomics and the integrin adhesome. Current Opinion in Cell Biology 24(5), 562-568.

Giaever, I., Keese, C.R., 1991. Micromotion of mammalian cells measured electrically. Proceedings of the National Academy of Sciences 88(17), 7896-7900.

Giaever, I., Keese, C.R., 1993. A morphological biosensor for mammalian cells. Nature 366(6455), 591-592.

Higashiyama, T., Katsuyama, A., Otori, H., Kamimura, T., Uehara, A., Kainuma, M., Takumi, R., Kudo,

Y., Ebina, M., Mochitate, K., Kon, T., Furuya, Y., Kikuchi, H., 2014. Detection of cellular damage by hydrogen peroxide using SV40-T2 cells on shear horizontal surface acoustic wave (SH-SAW) sensor. Ultrasonics 54(6), 1430-1438.

Li, F., Wang, J.H.C., Wang, Q.-M., 2008. Thickness shear mode acoustic wave sensors for characterizing the viscoelastic properties of cell monolayer. Sensors and Actuators B: Chemical 128(2), 399-406.

Liu, Q., Wu, C., Cai, H., Hu, N., Zhou, J., Wang, P., 2014. Cell-Based Biosensors and Their Application in Biomedicine. Chemical Reviews 114(12), 6423-6461.

Matatagui, D., Moynet, D., Fernández, M.J., Fontecha, J., Esquivel, J.P., Gràcia, I., Cané, C., Déjous, C., Rebière, D., Santos, J.P., Horrillo, M.C., 2013. Detection of bacteriophages in dynamic mode using a Love-wave immunosensor with microfluidics technology. Sensors and Actuators B: Chemical 185(0), 218-224.

Montagut, Y.J., García, J.V., Jiménez, Y., March, C., Montoya, A., Arnau, A., 2011. Frequency-shift vs phase-shift characterization of in-liquid quartz crystal microbalance applications. Review of Scientific Instruments 82(6), -.

Nowacki, L., Follet, J., Vayssade, M., Vigneron, P., Rotellini, L., Cambay, F., Egles, C., Rossi, C., 2015. Real-time QCM-D monitoring of cancer cell death early events in a dynamic context. Biosensors and Bioelectronics 64(0), 469-476.

Otori, H., Higashiyama, T., Uehara, A., Kainuma, M., Kudo, Y., Kamimura, T., Kon, T., Mochitate, K., Kikuchi, H., Furuya, Y., 2013. Signal change of surface acoustic wave (SAW) caused by H2O2 damage to SV40-T2 cells cultivated on SH-SAW sensor. Sensors and Actuators A: Physical 200(0), 162-167.

Racz, Z., Cole, M., Gardner, J.W., Pathak, S., Jordan, M.D., Challiss, R.A.J., 2011. Cell-based surface acoustic wave resonant microsensor for biomolecular agent detection. Solid-State Sensors, Actuators and Microsystems Conference (TRANSDUCERS), 2011 16th International, pp. 2168-2171.

Rocha, M.I.G., Jiménez, Y., Laurent, F.A., Arnau, A., 2013. Love Wave Biosensors: A Review.

Saitakis, M., Gizeli, E., 2012. Acoustic sensors as a biophysical tool for probing cell attachment and cell/surface interactions. Cell. Mol. Life Sci. 69(3), 357-371.

Saitakis, M., Tsortos, A., Gizeli, E., 2010. Probing the interaction of a membrane receptor with a surface-attached ligand using whole cells on acoustic biosensors. Biosensors and Bioelectronics 25(7), 1688-1693.

Sassolas, A., Hayat, A., Catanante, G., Marty, J.-L., 2013. Detection of the marine toxin okadaic acid: Assessing seafood safety. Talanta 105(0), 306-316.

Tang, A.X.J., Pravda, M., Guilbault, G.G., Piletsky, S., Turner, A.P.F., 2002. Immunosensor for okadaic acid using quartz crystal microbalance. Analytica Chimica Acta 471(1), 33-40.

van Meerloo, J., Kaspers, G.L., Cloos, J., 2011. Cell Sensitivity Assays: The MTT Assay. In: Cree, I.A. (Ed.), Cancer Cell Culture, pp. 237-245. Humana Press.

Wegener, J., Janshoff, A., Galla, H.J., 1998. Cell adhesion monitoring using a quartz crystal microbalance: comparative analysis of different mammalian cell lines. Eur Biophys J 28(1), 26-37.

Wegener, J., Janshoff, A., Steinem, C., 2001. The quartz crystal microbalance as a novel means to study cell-substrate interactions In situ. Cell Biochem Biophys 34(1), 121-151.

Wegener, J., Seebach, J., Janshoff, A., Galla, H.-J., 2000. Analysis of the Composite Response of Shear

Wave Resonators to the Attachment of Mammalian Cells. Biophysical Journal 78(6), 2821-2833.

Wei, X.-L., Mo, Z.-H., Li, B., Wei, J.-M., 2007. Disruption of HepG2 cell adhesion by gold nanoparticle and Paclitaxel disclosed by in situ QCM measurement. Colloids and Surfaces B: Biointerfaces 59(1), 100-104.

Wei, X.-L., Zhang, J., Mo, Z.-H., 2011. Regulation of chemokine receptor CXCR4 in HepG2 cell adhesion sensing by QCM. pp. 1317-1320. IEEE.

Wiese, M., D'Agostino, P.M., Mihali, T.K., Moffitt, M.C., Neilan, B.A., 2010. Neurotoxic Alkaloids: Saxitoxin and Its Analogs. Marine Drugs 8(7), 2185.

Xi, J., Chen, J., Garcia, M., Penn, L., 2013. Quartz crystal microbalance in cell biology studies. J Biochip Tissue chip S 5, 2153-0777.

Yicong, W., Ping, W., Xuesong, Y., Gaoyan, Z., Huiqi, H., Weimin, Y., Xiaoxiang, Z., Jinghong, H., Dafu, C., 2001. Drug evaluations using a novel microphysiometer based on cell-based biosensors. Sensors and Actuators B: Chemical 80(3), 215-221.

Zhang, X., Zou, Y., An, C., Ying, K., Chen, X., Wang, P., Sensitive detection of carcinoembryonic antigen in exhaled breath condensate using surface acoustic wave immunosensor. Sensors and Actuators B: Chemical(0).

Zhang, X., Zou, Y., An, C., Ying, K., Chen, X., Wang, P., 2014. A miniaturized immunosensor platform for automatic detection of carcinoembryonic antigen in EBC. Sensors and Actuators B: Chemical 205(0), 94-101.

Zou, L., Hu, N., Zhou, J., Su, K., Wang, Q., Du, L., Wu, C., Zhao, L., Wang, P., 2014. A Novel Electrical Cell-Substrate Impedance Biosensor for Rapid Detection of Marine Toxins. Sensor Letters 12(6-7), 1041-1045.

Illustration of figures

Fig. 1. Construction of the cell-based Love Wave biosensor. (a) Top and cross-sectional views of Love Wave sensor chip. (b) The 8-channel Love Wave detection system.

Fig. 2. (a) Structure of the PDMS cell culturing chamber. (b) Picture of the fixation of the PDMS chip onto the sensor surface.

Fig. 3. Real-time sensor responses to various cell seeding densities: (a) insertion loss variations; (b) phase shifts; Relationship between the initial seeding density and sensor response: (c) insertion loss variations; (d) phase shifts. All the data in (c) and (d) are represented in the form of means ± SD, n=5.

Fig. 4. The microscopic images of HepG2 cells at 24 on the sensor surface with different initial cell seeding densities.

Fig. 5. (a) Real-time insertion loss variation curves of both the test group (200 μg/L OA) and control group (fresh medium) during the detection process. (b) The normalized curves of HepG2 cells responding to various concentrations of OA (10, 20, 40, 60, 100, 150 and 200 μg/L). (c) Relationship between the OA concentration and insertion loss variations caused by OA. All the data in (c) and (d) are represented in the form of means ± SD, n=3.

Fig. 6. (a) Real-time insertion loss detection curves of HepG2 cells responding to 100 μg/L OA, 100 μg/L STX, 100 μg/L PbTx-3 and fresh medium. (b) The normalized curves of HepG2 cells responding to 100 μg/L OA, 100 μg/L STX, 100 μg/L PbTx-3 and fresh medium. (c) Comparison of the insertion loss variations after treated with 100 μg/L OA, 100 μg/L STX, 100 μg/L PbTx-3 and fresh medium. All data in (c) are represented in the form of means ± SD, n=3.

Figure 1

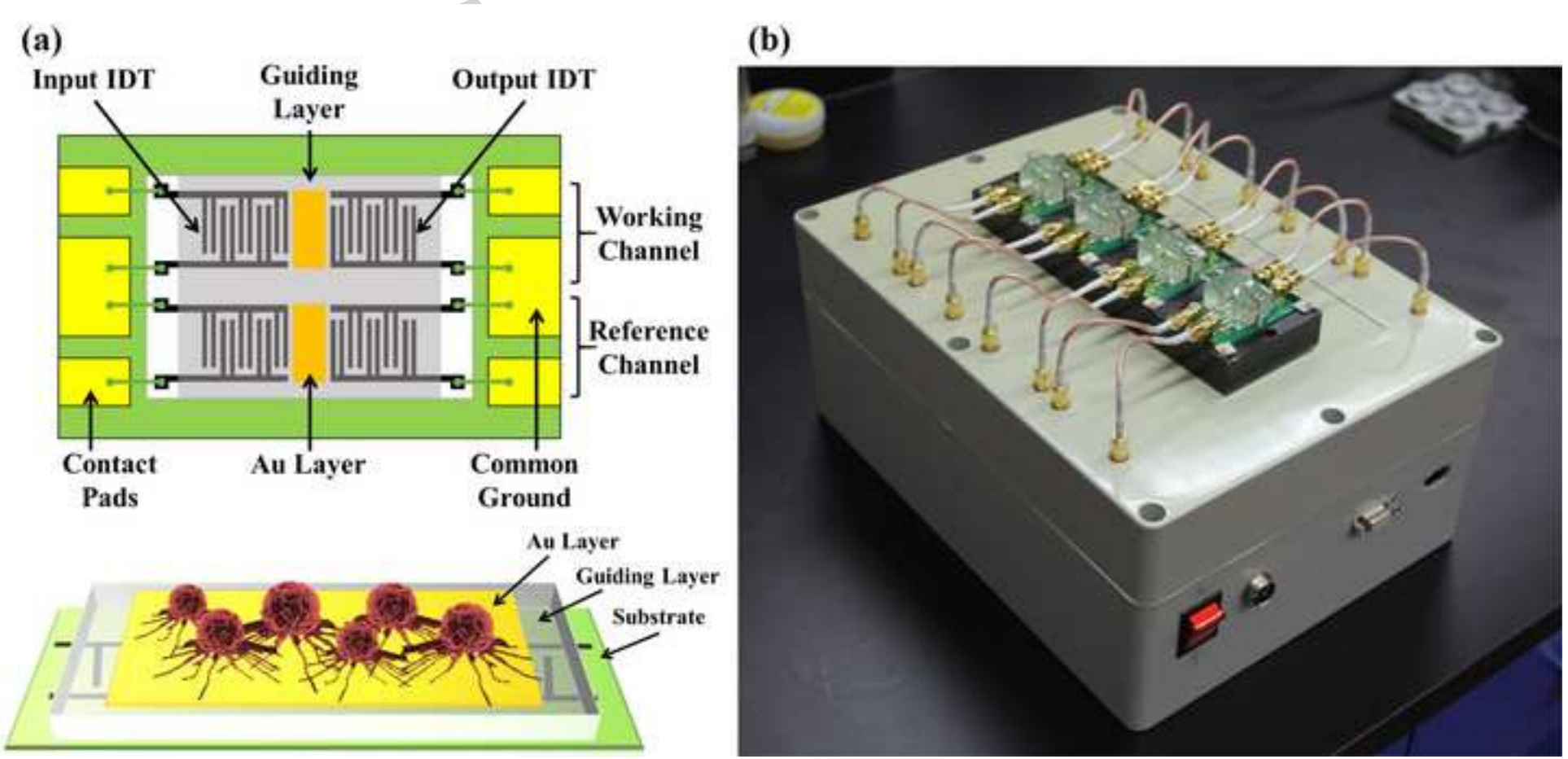

Figure 2

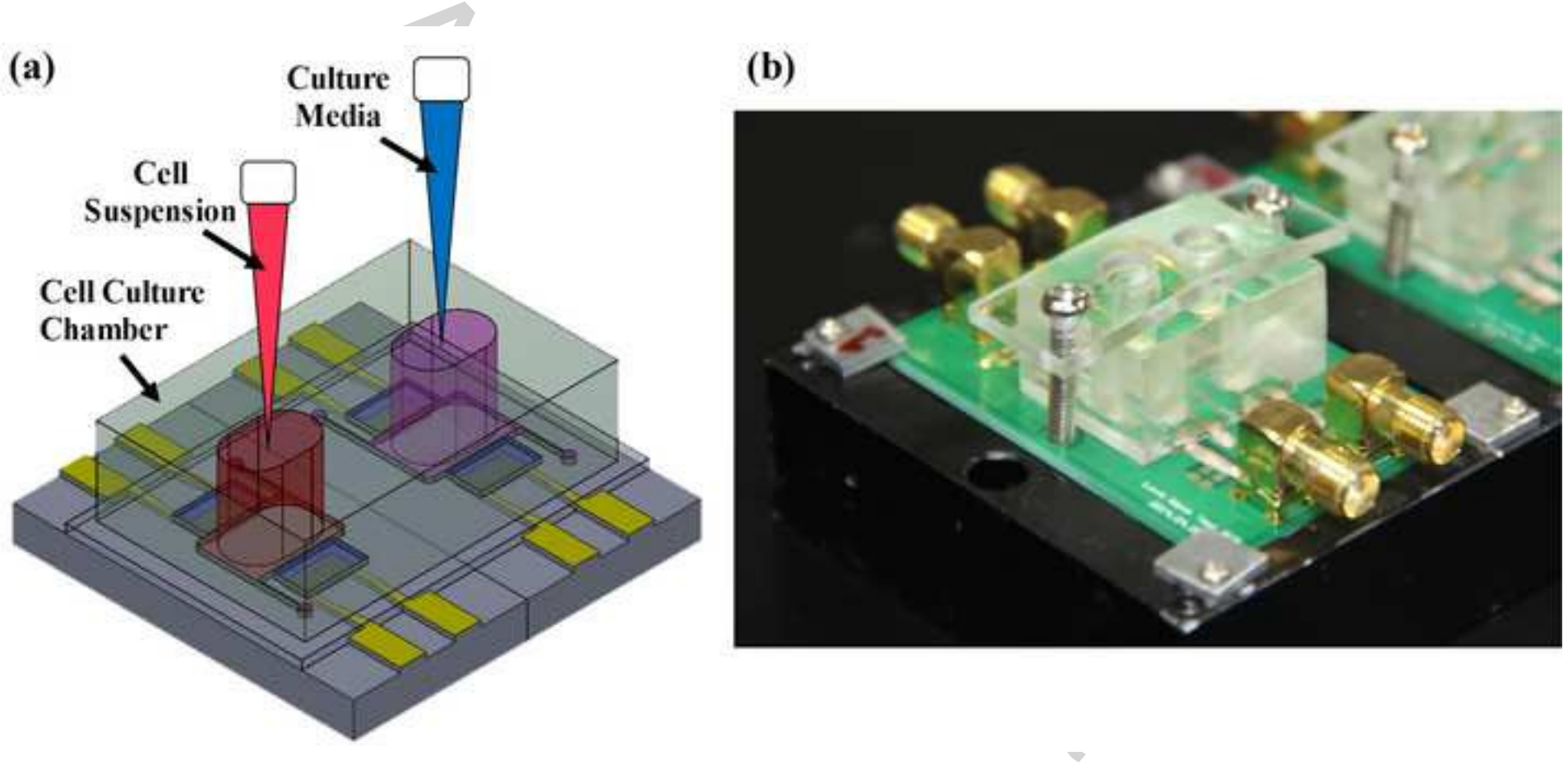

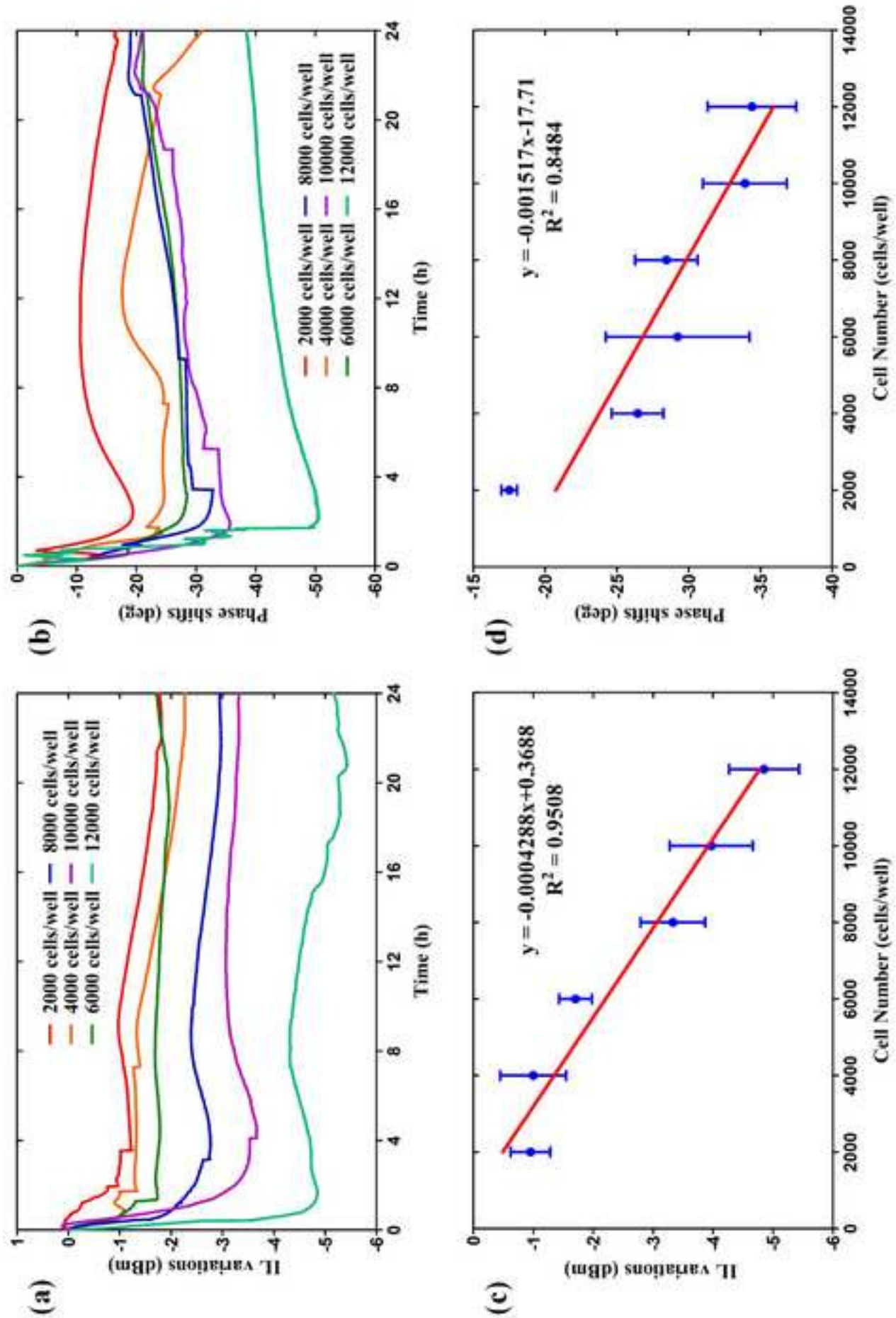
(a)
IL variations (dBm)
Time (h)
2000 cells/well
4000 cells/well
6000 cells/well
8000 cells/well
10000 cells/well
12000 cells/well
(b)
Phase shifts (deg)
Time (h)
2000 cells/well
4000 cells/well
6000 cells/well
8000 cells/well
10000 cells/well
12000 cells/well
(c)
IL variations (dBm)
Cell Number (cells/well)
y = -0.0004288x+0.3688
R² = 0.9508
(d)
Phase shifts (deg)
Cell Number (cells/well)
y = -0.001517x-17.71
R² = 0.8484

Figure 3

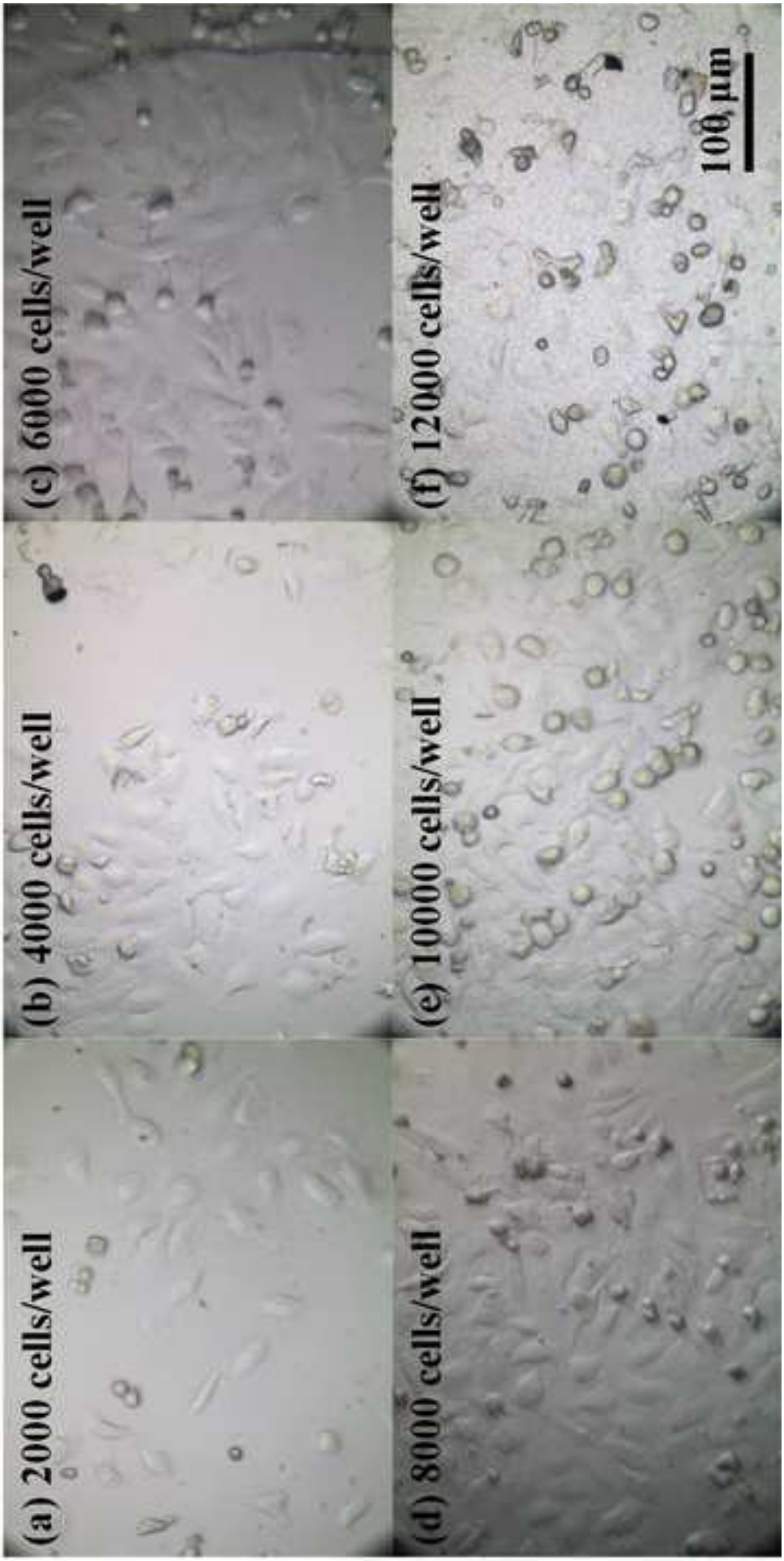
(a) 2000 cells/well
(b) 4000 cells/well
(c) 6000 cells/well
(d) 8000 cells/well
(e) 10000 cells/well
(f) 12000 cells/well
100 µm

Figure 4

Figure 5

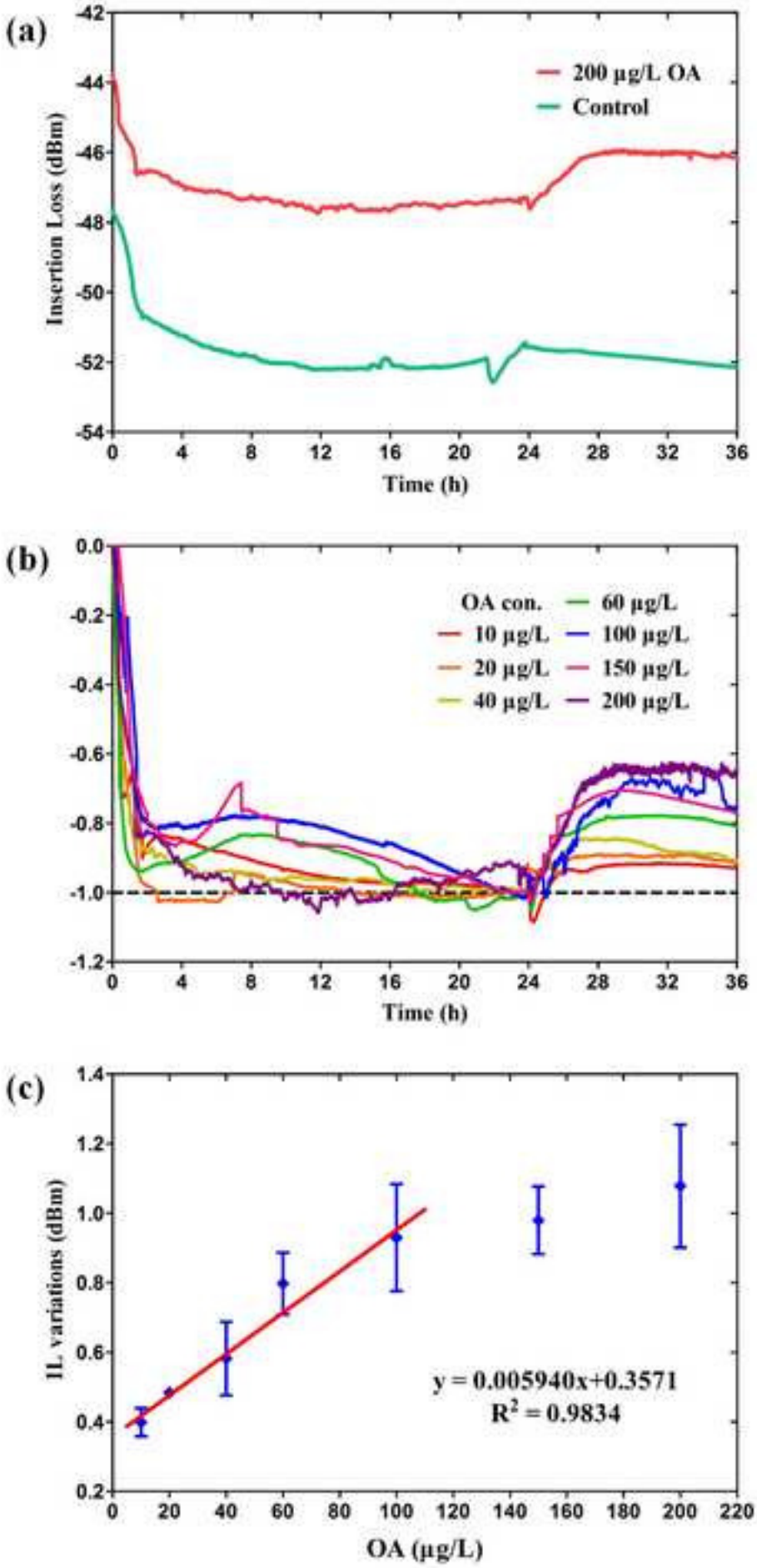

Figure 6